Generalized Gamma Distribution SAR Sea Clutter Modelling for Oil Spill Candidates Detection

Mari-Cortes Benito-Ortiz, David Mata-Moya, Maria-Pilar Jarabo-Amores
Nerea del Rey-Maestre and Pedro-Jose Gomez-del-Hoyo
Signal Theory and Communications Department
Superior Polytechnic School. University of Alcalá
Alcalá de Henares, Madrid, Spain
e-mail: {cortes.benito, david.mata, mpilar.jarabo, nerea.rey, pedrojose.gomez}@uah.es

***Abstract*—This paper tackles the oil spills offshore monitoring using satellite Earth Observation tools based on Synthetic Aperture Radar (SAR) sensors. The proposed processing scheme is based on modelling SAR sea backscattering assuming a Generalized Gamma Distribution clutter. The signal processing scheme includes a first stage to define the non-homogeneous area due to the presence of dark spots in function of the multi-scale estimations of a textural parameter defined as the inverse of the product between shape and scale sea clutter parameters. After an statistical study of this parameter, a robust value can be defined for comparison purposes. In the resulted search area, an adaptive thresholding is performed to obtain a segmented image with the oil slicks candidates contouring at pixel level. Results obtained with SAR images acquired by Sentinel-1 over Corsica, confirm the suitability of the proposed methodology.**

***Index Terms*—SAR, Oil Spill, Generalized Gamma Distribution, Radar Detection**

I. Introduction

Offshore oil pollution has become one of the major marine disasters causing great harm to the marine ecology. The oil slicks detection is very important as early as possible to reduce the damage to the wildlife and to provide significant assistance to eliminate emergency situations. The source of oil spills can be both natural leaks and human accidents on fixed and moving tankers or refineries. Remote sensing tools using geoinformation systems are considered for monitoring oil spill with reliability [1], [2]. This paper is focused on satellite Earth Observation (EO) Synthetic Aperture Radars (SAR) Sensors due to their capability of providing high-resolution imagery acquired under any weather and light condition [3].

In SAR imagery, offshore oil spill candidates can be detected indirectly as a capillary waves dampening effect shown as dark spots. These spots can also be caused by other natural phenomena named look-alikes: natural film, grease ice, threshold wind, algae blooms, rain cells, internal waves, current shear zones or natural seepage, grease ice,... [4], [5].

The scheme for oil spill monitoring is usually composed of dark formations detection, features extraction, false alarm discrimination and classification. The first step is critical and fundamental, because once oil spills are omitted in this stage, they will never be detected in later steps. Furthermore, the performance accuracy of feature extraction greatly rely on dark spot detection capabilities. In manual detection, a trained operator find possible oil spills in the entire image, but it is labor-intensive and time-consuming. Thus, fast, reliable and automated oil-spill detection systems have been developed. For example, the use of wavelets, fractal dimension estimation, segmentation-based methods and mathematical morphology have been considered [6]–[9]. However, the intensity threshold-based algorithm is a common approach used due to its computational efficiency. In [10], [11], a global thresholding for the entire image is proposed. On the other hand, strategies to fix adaptive thresholds attending to estimations of local statistics properties in a moving window have been considered [12]–[14]. However, the proposed statistical parameters are not related with a clutter model that fit with variations of SAR data associated with sea echoes. In addition, the performance of a detector implemented at pixel level is characterized by a huge number of false alarms, because SAR data is highly speckled and low backscatter pixel values can be associated with sea clutter, ground clutter, oil slicks or look-alikes.

In this paper, the dark spot detection is design in a two-stage scheme: the first one deals with the identification, in the entire image, of non-homogeneous areas where dark spots can be present; the second one consists of an adaptive thresholding. Both stages consider a statistical model based on Gamma Generalized Distribution (GΓD) for high-resolution SAR sea-clutter [15], [16]. Statistical characterization of SAR data acquired in an offshore area is carried out to study the behavior of the GΓD parameters with and without oil slicks. Attending to the complexity of SAR imagery automatic interpretation, local statistical estimations at multiple scales are considered [17]. After the multi-scale comparative study, an homogeneity indicator for the first stage is defined. Finally, an adaptive threshold is fixed attending to Probability False Alarm (P_{FA}) requirements and local estimations of GΓD parameters.

The proposed solution is validated using SAR images acquired by Sentinel-1 [18], a side-looking C-band SAR sensor, during the disaster caused by the collision with a tanker near Cap Corse on October 2018. Geo-referenced results confirm the ability of this solution to map oil slicks candidates.

II. Oil Spill Candidates Detector

The methodology proposed to segment out oil spill candidates in SAR imagery is based on a GΓD clutter model.

978-9-0827-9703-9/19/$31.00 ©2019 IEEE

Local estimations of the corresponding statistical parameters are carried out to identify the search area of dark spots and to determine an adaptive threshold to maintain a constant P_{FA}. The considered processing stages reduce isolated false alarms in the entire image and provide an accuracy detection performance for later feature extraction. The design details and selected parameters of the algorithm implementation are described in sections III-B and III-C.

A. Generalized Gamma Distribution Clutter Model

It is widely extended the assumption of a Gaussian model for the SAR sea clutter in thresholding algorithms that had the goal been just the detection of a dark area [12], [13], [19]; however, in the spirit of making the most of the high-resolution SAR sensors can achieve, deeper statistical characterization can be considered [15], [16], [20]–[23]. In [24], the suitability of the GΓD, a heavy-tailed distribution, for modelling the high variability of SAR sea clutter is proved.

The probability density function, PDF, and the cumulative distribution function,CDF, of GΓD are defined in equations (1) and (2), respectively.

$$p(x|k,\nu,\sigma) = \frac{k^k \nu}{\sigma \Gamma(k)} \left(\frac{x}{\sigma}\right)^{k\nu-1} e^{-k\left(\frac{x}{\sigma}\right)^{\nu}} \tag{1}$$

$$C(x|k,\nu,\sigma) = \frac{\gamma\left(k, \left(\frac{x}{k^{\nu}\sigma}\right)^{\nu}\right)}{\Gamma(k)} \tag{2}$$

$\Gamma()$ denotes the Gamma function, $\gamma()$ the lower incomplete Gamma function. The associated statistical parameters are: $k > 0$ the shape one, $\sigma > 0$ the scale one, and $\nu \neq 0$ the power one. GΓD can model both amplitude and intensity fluctuations and has several special cases: Rayleigh ($\nu = 2$, $k = 1$), exponential ($\nu = 1$, $k = 1$), Nakagami ($\nu = 2$), Gamma ($\nu = 1$), lognormal ($k \to \infty$) and Weibull ($k = 1$).

B. Search Area of Dark Spots

The objective of this stage is the definition of a homogeneity indicator based on a local texture measurement that can be used for identify areas where dark formations can appear in spite of speckle contamination. Attending to a multi-scale strategy, the homogeneity indicator is estimated for different window sizes for improving the characterization of the SAR textural information [17].

In [12], [14], [25], Power-to-Mean Ratio (PMR) is considered as homogeneity indicator and is used for detection and classification purposes. However, the values of PMR associated with oil slicks are speckle dependent varying from one SAR image to another and the selection of predefined values is a very complex task.

In this paper, statistical characterization of sea clutter is considered and GΓD parameters are estimated using Mellin transform [26] in areas with and without oil spills. After studying the behavior of the statistical parameters separately and combined, a new robust homogeneity indicator (H) is proposed. To discover the search area, a statistical characterization of H values is carried out with the available SAR database.

C. Dark Spots Declaration

An adaptive amplitude thresholding technique is implemented in the defined search area of dark spots:

- After applying a land mask, the entire sea area is divided into equally-sized patches, selected as a compromise solution between controlling the estimation error and maintaining the local characterization of sea clutter.
- For each patch, only data outside the previously defined search area by H measurements are used as sea clutter for GΓD parameters etimation using Mellin transform [26].
- A local amplitude threshold fixed attending to P_{FA} requirements, providing a good insight into the different states of the sea.
- The adaptive threshold is applied not in the whole patch but in the declared search area to detect dark pixels that can belong to dark formations.

This scheme detects at pixel level, so morphological operations are required to connect nearby detections and forming the finally declared dark spots. These operations consider the typical slick shapes: narrow or tail slicks (straight or slightly bent depending on the weather conditions history) and wide slicks (with a not clear delineation and a difficult relation with wind temporal data) [27], [28]. The final output is a binary segmented image where the dark spots, regardless their shape, are stand out clearly and can be used to obtain an accuracy performance of the later feature extractor.

III. Results

A. SAR Images Database

On the morning of 7th October 2018, the Tunisian vessel Ulysse collided with the Cypriot container ship CSL Virginia anchored in the open sea some 28 km north of Cap Corse. Bunker fuel immediately began to leak out and the pollution spread over around 25 km forming distinct slicks in a northwesterly direction. Two SAR images acquired by C-Band Sentinel-1 in the following two days have been considered to evaluate the proposed solution (Figures 1(a) and 2(a)). In Table I, the corresponding acquisition parameters and main image properties are detailed. In Figures 1(b) and 2(b), the respective zoomed areas containing the oil slicks are depicted. In Fig. 1(b), the selected areas of sea clutter with (highlighted in green) and without (highlighted in red) oil slicks for the statistical modelling are shown.

TABLE I
Relevant information about SAR Images Database

	Image 1 (Fig. 1(a))	**Image 2 (Fig. 2(a))**
Acquisition Mode	Interferometric Wide Swath	
Product Type	Ground Range Detected	
Polarization	VV	
Acquisition Day	2018-10-08	2018-10-09
Wind Intensity	3.5 m/s	2.5 m/s
Wind Direction	135°	147°
Pixel Spacing	10m x 10m	
Illuminated Area	166.73km x 264km	167.02km x 259.74km

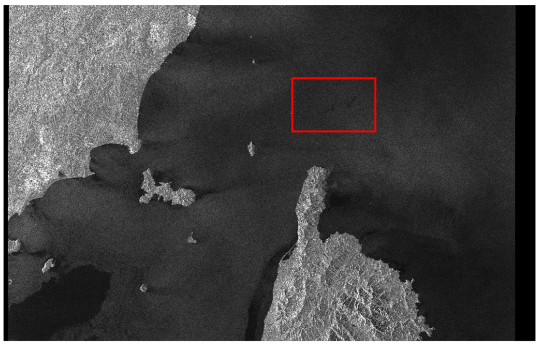

(a) SAR GRD product

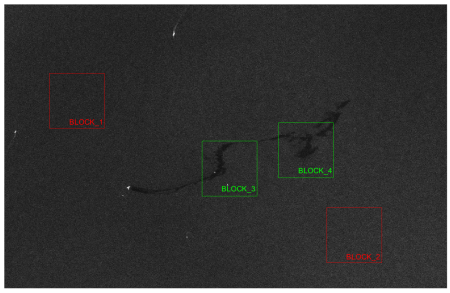

(b) Zoomed area

Fig. 1. SAR image 1 acquired by Sentinel-1 acquired on 8th October

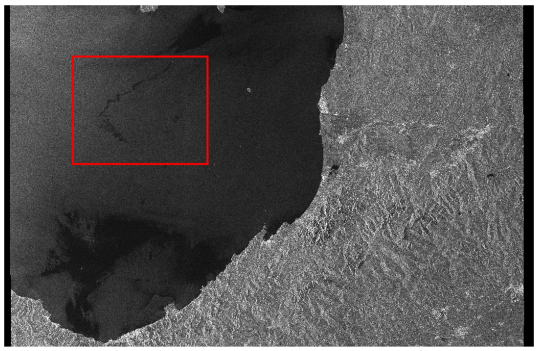

(a) SAR GRD product

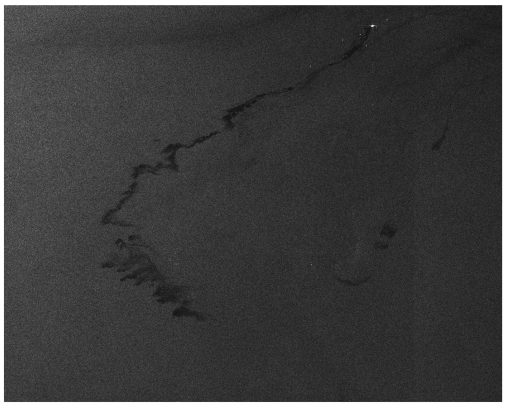

(b) Zoomed area

Fig. 2. SAR image 2 acquired by Sentinel-1 acquired on 9th October

B. Homogeneity Indicator Definition

Statistical modelling of amplitude variation of SAR data highlighted in the blocks of Fig. 1(b), after the brightest pixels of each block have been filtered to ensure that the remaining pixels belong mostly exclusively to the sea surface, is carried out. The estimated statistical parameters of GΓD are summarized in Table II, including the root mean square error (RMSE) of the empirical PDF ($p_e(x)$) with respect to the theoretical one ($p_t(x)$) formulated with the corresponding GΓD parameters as a metric measurement. The RMSE is calculated with the expression (3) where N is the number of generic points (bins) on the amplitude axis in which both PDFs are evaluated. Similar RMSE values confirm that GΓD clutter is so suitable for modelling sea clutter with oil slicks as without them.

$$RMSE = \sqrt{\frac{1}{N}\sum_{n=0}^{N} |p_e(x) - p_t(x)|^2} \tag{3}$$

TABLE II
STATISTICAL PARAMETERS OF SAR SEA CLUTTER MODELED AS GΓD

	k	ν	σ	$1/(k \cdot \nu)$	RMSE
Block_1	1.7211	8.1955	0.3320	0.0709	10.3722
Block_2	1.8212	7.6044	0.3495	0.0722	10.3456
Block_3	1.5322	7.9272	0.3314	0.0823	10.8872
Block_4	1.8007	6.1963	0.3396	0.0896	9.1590

Any trend can be concluded about the dependence of the GΓD parameters with the presence of dark spots, but an homogeneity indicator (H) can be defined in function of the shape and scale parameters: $H = 1/(k \cdot \nu)$. H values are also detailed in Table II, and it is shown that H is higher when the modeled sea clutter data contain oil slicks.

H is locally estimated in blocks of 512x512, 256x256, 128x128 and 64x64 pixels. H_P will denote the H estimated in blocks consisting of P rows and P columns. In Fig. 3, PDFs of H_P values are depicted. Regardless P value, there are more probable H values associated with non polluted sea clutter. In addition, a threshold value can be defined to identify the non-homogeneous areas ($H > 0.08$). As this parameter only depends on k and ν, avoiding σ that is less robust against speckle noise, the threshold value can be extrapolated to other SAR data acquisition conditions.

A multi-scale strategy is implemented in different iterations: in the first one, blocks whose $H_{512} > 0.08$ are labelled as search area of dark spots; the following iterations are performed over the remaining area taking decisions at different scales comparing H_{256}, H_{128} and H_{64} estimations, respectively, with the threshold value of 0.08.

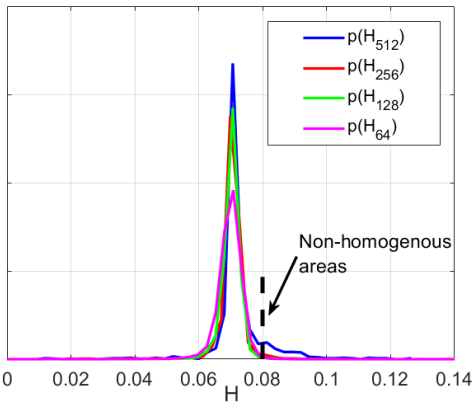

Fig. 3. PDFs of H_P values

C. Oil Spill Candidates Detector Performance

In Fig. 4(a), the search area of dark spots associated with the SAR Image 1 is presented. Results confirm the proposed multi-resolution algorithm based on H to stand out the non-homogeneous areas. In Fig. 4(b), the detection capability of the adaptive threholding using local estimation of GΓD parameters is shown. 6 dark spots are declared and the considered detector at pixel-level fits quite well with the oil spills allowing an accuracy performance of the later feature extractor.

To confirm the robustness of the proposed scheme, results obtained for Image 2 are depicted in Figures 5(a) and 5(b). The search area is well defined using different scales and the threshold value $H_P > 0.08$ (Fig. 5(a)). In this second day after the collision, 17 oil spill candidates are detected (Fig. 5(b)).

Geo-referenced results of two images are presented over Google Earth to monitor the pollution. In both images, tail oil formations, with an orientation close to wind direction conditions, are detected near the point source. In the second image, the pollution is extended and wider oil slicks shapes with a not clear delineation are detected.

IV. Conclusions

In this paper, an oil spill candidates detector based on GΓD clutter for modeling variations of sea echoes in SAR imagery. SAR systems are suitable EO tools, although the automatic interpretation is a complex task. Oil spills on SAR images appear as dark spots, although other phenomena can give false oil spill positives or look-alikes.

The proposed processing scheme is based on local and multi-scale estimations of GΓD clutter parameters in the entire SAR image. The proposed scheme is composed by the identification of the search area, where dark spots can be contained, and an adaptive thresholding. The output is a segmented image with the oil spill candidates contouring at pixel level for improving the feature extraction.

After an statistical study of sea clutter patches with and without dark formations, an homogeneity indicator (H) is defined as the inverse of the product between the shape and the scale GΓD parameters. Higher values of H are associated

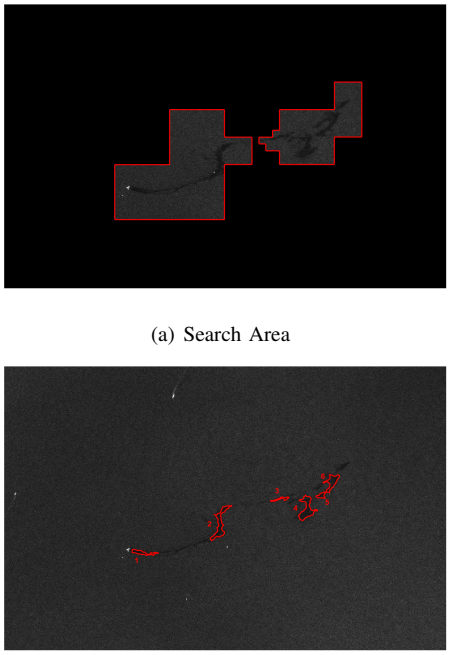

(a) Search Area

(b) Detected Dark Spots

Fig. 4. Oil Spill Candidates Detector Performance for the zoomed area of SAR Image 2 (Fig. 1(b))

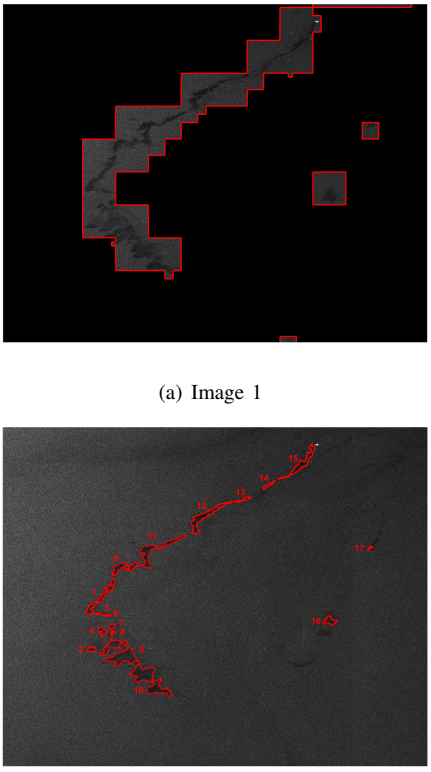

(a) Image 1

(b) Image 2

Fig. 5. Oil Spill Candidates Detector Performance for the zoomed area of SAR Image 1 (Fig. 2(b))

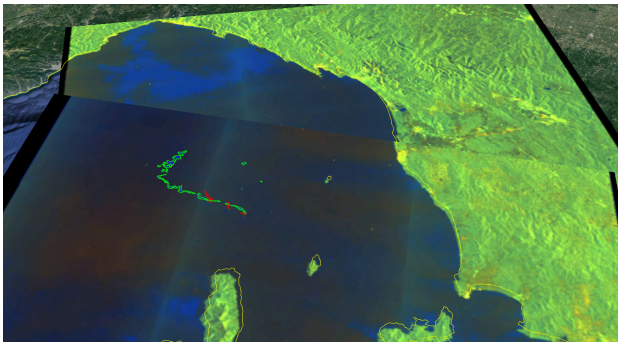

Fig. 6. Monitoring of the georreferenced oil spill candidates over Google Earth

with non-homogeneous areas and, as H is not dependent of the speckle noise level and also the estimation resolution, a threshold value can be prefixed. The proposed methodology is implemented in four iterations, one for each considered block size, labelling the blocks where $H_P > 0.08$ as the search area. The detector of dark pixels is based on a threshold fixed attending to the desired P_{FA} and the formulated GΓD CDF with local estimations of clutter parameters. Only data outside the search area is considered for this estimations, although the adaptive thresholding is only applied to the search area.

The designed algorithm is evaluated with SAR images acquired by Sentinel-1 after the collision and oil spill off Corsica. Oil spill candidates with different shapes are detected confirming the suitability of the proposed technological solution for monitoring pollution disasters.

ACKNOWLEDGMENT

This work has been partially funded by the Spanish "Ministerio de Economía, Industria y Competitividad" under projects TEC2015-71148-R and RTI2018-101979-B-I00.

REFERENCES

[1] M. Fingas and C. Brown, "Review of oil spill remote sensing," *Marine Pollution Bulletin*, vol. 83, no. 1, pp. 9 – 23, 2014.

[2] A. V. Agadilov, N. I. Kurakina, and A. D. Kuzmina, "The modeling of emergency oil spills in gis," in *2018 IEEE Conference of Russian Young Researchers in Electrical and Electronic Engineering (EIConRus)*, Jan 2018, pp. 1187–1189.

[3] J. C. Curlander and R. N. McDonough, *Synthetic Aperture Radar: Systems and Signal Processing*. Wiley-Interscience, 1991.

[4] C. Brekke and A. H. Solberg, "Oil spill detection by satellite remote sensing," *Remote Sensing of Environment*, vol. 95, no. 1, pp. 1 – 13, 2005.

[5] A. Pisano, M. D. Dominicis, W. Biamino, F. Bignami, S. Gherardi, F. Colao, G. Coppini, S. Marullo, M. Sprovieri, P. Trivero, E. Zambianchi, and R. Santoleri, "An oceanographic survey for oil spill monitoring and model forecasting validation using remote sensing and in situ data in the mediterranean sea," *Deep Sea Research Part II: Topical Studies in Oceanography*, vol. 133, pp. 132 – 145, 2016, physical, chemical and biological observations and modelling of oil spills in the Mediterranean Sea.

[6] S. Derrode and G. Mercier, "Unsupervised multiscale oil slick segmentation from sar images using a vector hmc model," *Pattern Recognition*, vol. 40, no. 3, pp. 1135 – 1147, 2007.

[7] F. Berizzi, M. Martorella, G. Bertini, A. Garzelli, F. Nencini, F. Dell'Acqua, and P. Gamba, "Sea sar image analysis by fractal data fusion," in *IGARSS 2004. 2004 IEEE International Geoscience and Remote Sensing Symposium*, vol. 1, Sept 2004, p. 96.

[8] Y. Shu, J. Li, H. Yousif, and G. Gomes, "Dark-spot detection from sar intensity imagery with spatial density thresholding for oil-spill monitoring," *Remote Sensing of Environment*, vol. 114, no. 9, pp. 2026 – 2035, 2010.

[9] A. Gasull, X. Fábregas, J. Jiménez, F. Marqués, V. Moreno, and M. A. Herrero, "Oil spills detection in sar images using mathematical morphology," in *2002 11th European Signal Processing Conference*, Sep. 2002, pp. 1–4.

[10] F. Nirchio, M. Sorgente, A. Giancaspro, W. Biamino, E. Parisato, R. Ravera, and P. Trivero, "Automatic detection of oil spills from sar images," *International Journal of Remote Sensing*, vol. 26, no. 6, pp. 1157–1174, 2005.

[11] L. Chang, Z. Tang, S. Chang, and Y.-L. Chang, "A region-based glrt detection of oil spills in sar images," *Pattern Recognition Letters*, vol. 29, no. 14, pp. 1915 – 1923, 2008.

[12] A. H. S. Solberg, C. Brekke, and P. O. Husoy, "Oil spill detection in radarsat and envisat sar images," *IEEE Transactions on Geoscience and Remote Sensing*, vol. 45, no. 3, pp. 746–755, March 2007.

[13] X. M. Li, T. Jia, and D. Velotto, "Spatial and temporal variations of oil spills in the north sea observed by the satellite constellation of terrasar-x and tandem-x," *IEEE Journal of Selected Topics in Applied Earth Observations and Remote Sensing*, vol. 9, no. 11, pp. 4941–4947, 2016.

[14] M.-C. Benito-Ortiz, D. Mata-Moya, M.-P. Jarabo-Amores, M. Maganto-Pascual, and P.-J. Gomez-del Hoyo, *Multi-resolution Technique-Based Oil Spill Look-Alikes Detection in X-Band SAR Data: ICICT 2018, London*, 01 2019, pp. 737–745.

[15] W. Ao, F. Xu, Y. Li, and H. Wang, "Detection and discrimination of ship targets in complex background from spaceborne alos-2 sar images," *IEEE Journal of Selected Topics in Applied Earth Observations and Remote Sensing*, vol. 11, no. 2, pp. 536–550, Feb 2018.

[16] J. M. de Nicolás, P. Jarabo-Amores, N. Rey-Maestre, D. Mata-Moya, and J. L. Bárcena-Humanes, "A non-parametric cfar detector based on sar sea clutter statistical modeling," in *2015 IEEE International Conference on Image Processing (ICIP)*, Sept 2015, pp. 4426–4430.

[17] G. D. Grandi, D. Hoekman, J. S. Lee, D. Schuler, and T. Ainsworth, "A wavelet multiresolution technique for polarimetric texture analysis and segmentation of sar images," in *IGARSS 2004. 2004 IEEE International Geoscience and Remote Sensing Symposium*, vol. 1, Sept 2004, p. 713.

[18] ESA, "Sentinel-1 mission. http://sentinel.esa.int/web/sentinel," 2018.

[19] B. Lounis and A. B. Aissa, "A contextual segmentation of sea sar images to detect dark spots in mediterranean sea," in *2006 2nd International Conference on Information Communication Technologies*, vol. 1, 2006, pp. 371–376.

[20] M. Greco, F. Gini, and M. Rangaswamy, "Statistical analysis of measured polarimetric clutter data at different range resolutions," *IEE Proceedings - Radar, Sonar and Navigation*, vol. 153, no. 6, pp. 473–481, 2006.

[21] M. S. Greco and F. Gini, "Statistical analysis of high-resolution sar ground clutter data," *IEEE Transactions on Geoscience and Remote Sensing*, vol. 45, no. 3, pp. 566–575, 2007.

[22] A. Farina, F. Gini, M. V. Greco, and L. Verrazzani, "High resolution sea clutter data: statistical analysis of recorded live data," *IEE Proceedings - Radar, Sonar and Navigation*, vol. 144, no. 3, pp. 121–130, 1997.

[23] K. J. Sangston, F. Gini, and M. S. Greco, "Coherent radar target detection in heavy-tailed compound-gaussian clutter," *IEEE Transactions on Aerospace and Electronic Systems*, vol. 48, no. 1, pp. 64–77, 2012.

[24] J. Martín-de Nicolás, M.-P. Jarabo-Amores, D. Mata-Moya, N. del Rey-Maestre, and J.-L. Bárcena-Humanes, "Statistical analysis of sar sea clutter for classification purposes," *Remote Sensing*, vol. 6, no. 10, pp. 9379–9411, 2014.

[25] C. Brekke and A. H. S. Solberg, "Classifiers and confidence estimation for oil spill detection in envisat asar images," *IEEE Geoscience and Remote Sensing Letters*, vol. 5, no. 1, pp. 65–69, Jan 2008.

[26] H.-C. Li, W. Hong, and Y.-R. Wu, "Generalized gamma distribution with molc estimation for statistical modeling of sar images," in *2007 1st Asian and Pacific Conference on Synthetic Aperture Radar*, 2007, pp. 525–528.

[27] K. N. Topouzelis, "Oil spill detection by sar images: Dark formation detection, feature extraction and classification algorithms," *Sensors*, vol. 8, no. 10, pp. 6642–6659, 2008.

[28] D. Mera, J. M. Cotos, J. Varela-Pet, and O. Garcia-Pineda, "Adaptive thresholding algorithm based on sar images and wind data to segment oil spills along the northwest coast of the iberian peninsula," *Marine Pollution Bulletin*, vol. 64, no. 10, pp. 2090 – 2096, 2012.